

# CTrGAN: Cycle Transformers GAN for Gait Transfer

Shahar Mahpod<sup>1</sup>, Noam Gaash<sup>1</sup>, and Gil Ben-Artzi<sup>1</sup>

Ariel University, Ariel , Israel  
{mahpods,noam.gaash,gilba}@ariel.ac.il

**Abstract.** We attempt for the first time to address the problem of gait transfer. In contrast to motion transfer, the objective here is not to imitate the source’s normal motions, but rather to transform the source’s motion into a typical gait pattern for the target. Using gait recognition models, we demonstrate that existing techniques yield a discrepancy that can be easily detected. We introduce a novel model, Cycle Transformers GAN (CTrGAN), that can successfully generate the target’s natural gait. CTrGAN’s generators consist of a decoder and encoder, both Transformers, where the attention is on the temporal domain between complete images rather than the spatial domain between patches. While recent Transformer studies in computer vision mainly focused on discriminative tasks, we introduce an architecture that can be applied to synthesis tasks. Using a widely-used gait recognition dataset, we demonstrate that our approach is capable of producing over an order of magnitude more realistic personalized gaits than existing methods, even when used with sources that were not available during training.

## 1 Introduction

The goal of motion transfer is to synthesize a video in which one individual is acting in accordance with that of a different individual in a given real video. A growing body of research has been conducted on this topic, which has led to the development of advanced detection [29,24,8] and enhanced motion transfer techniques [41,8]. As a result of their mutually reinforcing relationship, motion transfer technology can produce convincingly realistic images and videos through deep learning-based manipulations.

In this paper, we propose a novel approach for gait transfer. The goal is to replace a walking person (source) in a video sequence with photorealistic images of a different walking person (target), such that the resulting gait is identifiable as the target’s. Contrary to fingerprints or faces, gait is harder to conceal and can be detected from a distance, even without the cooperation of the subject. Consequently, the ability to replace individuals in surveillance videos, for example, may have considerable importance. Currently, there is no openly available dedicated gait transfer approach. Using the whole-body motion transfer approach [8] for gait transfer has the following key limitation: it attempts to replicate the precise movements of the source; rather, the goal of gait transfer



Fig. 1: CTrGAN transfers the poses of the source to the target, while maintaining the natural gait of the target. From left to right: (a) The source’s image (a woman) is converted to (b) DensePose’s [17] IUUV format. (c) Our model translates the IUUV of the source to the corresponding most natural IUUV pose of the target by synthesizing a novel pose. (d) The generated pose is very similar (but not identical) to an existing *real* pose in the dataset. (e) The generated pose is rendered to a corresponding RGB image of the target (a man).

is to translate the typical motions and appearances of the source into those of the target, adjusting for varied angles, paces, and shapes. Therefore, it is imperative to publicly disclose such a method, in order to allow for the emergence of corresponding detection methods in a timely manner.

We introduce CTrGAN for gait transfer. It transfers a series of poses from the source to the target while maintaining the natural movements of the target. Sources may vary in viewpoint, shape, and pace. It is based on Transformers [38], which have proven to be successful in translation tasks. Similar to NLP’s models [44,5], each Transformer consists of an encoder and a decoder. As a result, we can successfully translate between the sequences of poses of the sources and the targets. As opposed to previous Transformer models used in computer vision [12,46], our model performs self- and cross- attention in time rather than in image space, capturing the dynamic of the object. In order to generate unseen natural poses of the target, our model is trained in an unsupervised manner on unpaired data. This is in contrast to prior whole-body motion transfer approaches that required paired data (e.g., [40]). Figure 1 shows our method.

The quality of whole-body motion transfer is often evaluated in a supervised manner, based on the ability to approximate a pose and appearance of the target unseen during training but available in the test set. In our case, in addition to the appearance, the objective is to measure the translation of the gait pattern (i.e. the dynamic) from the source to a typical gait pattern of the target. In many cases, there are no one-to-one correspondences between each frame in the newly generated dynamic of the target and the existing ones already included in the dataset, and therefore it can not be evaluated directly in a supervised manner. We propose employing state-of-the-art gait recognition algorithms [34] to evaluate the quality of the gait transfer. The quality is determined by the accuracy with which newly generated poses are recognized as the target’s gait. In

order to provide accurate measurements in all scenarios, we use several different algorithms [9,14,25]. As a way of assessing the appearances of unseen poses, Chamfer’s distance is used.

Our model includes two networks: (a) CTrGAN, which translates the poses of the sources to the poses of the target, and (b) pose-to-appearance, which renders the appearance of each pose. For the latter network, we deploy an independent state-of-the-art existing approach.

This paper contributes by (a) making the first attempt at exploring the gait transfer problem and proposing gait recognition models as an evaluation and detection method; (b) introducing Cycle Transformers GAN with temporal attention that can generate realistic gait patterns of the targets, undetectable under existing gait recognition models; and (c) demonstrating the effectiveness of our approach based on a standard gait recognition dataset, showing that it can generalize to unknown input sources, yielding the desired gait in an order of magnitude more cases than previous methods.

## 2 Related work

**Pose-to-Appearance** A variety of methods have been introduced for the generation of video sequences of the target based on semantic input, including facial motion transfer [32,23,2,37] and whole-body motion transfer [8,10,40,41,28,45]. These methods are based on the ability to accurately estimate the pose [17,6] and also on image-to-image translation models [42,48]. They are either explicitly trained for each source [8] or can be trained only once [40] as our approach. In contrast to previous works, our goal is to generate the personalized gait pattern of the target to best match the gait of the source rather than to accurately imitate the original motion of the source. Building on the recent advances, we employ [8,41] as our pose-to-appearance network where the input is the generated poses of the target and not the source’s poses. Our experiments demonstrate the benefits of CTrGAN over the direct use of [8,41] for gait transfer.

**Gait Recognition.** In recent years, various works have been proposed that use neural network models to identify people based on their gait [9,14,36,11]. GaitSet [9] considers the gait as a set consisting of independent frames and recognizes it based on a sequence of silhouette images. GaitGL [25] relay on both global visual information and local region details and introduced attention between adjacent frames. GaitPart [14] uses a novel part-based model to characterize the gait. We use GaitSet, GaitGL, and GaitPart models to assess the quality of the generated video sequence. When the source in the video sequence is replaced with the target, the identified gait should be replaced as well. We show that for previous approaches, a gait is still readily associated with its source while using our approach it is considered to belong to the target.

**Visual Transformers.** Transformers [38] are proven architectures in the field of Natural Language Processing [5], and several works have been done

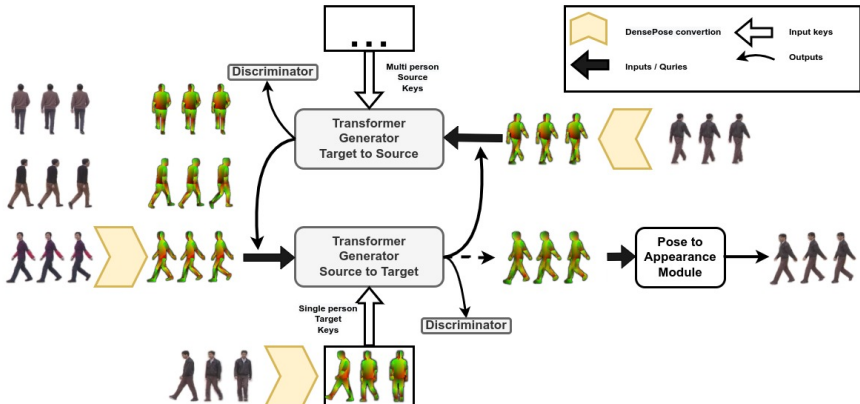


Fig. 2: The generators of CTGAN are based on transformers. The inputs to each generator are IUVA gait images from the training set and Keys. The outputs are natural gait poses. See the text for further details.

in recent years to adapt them to computer vision [26,12,19]. The Transformer model is shown in [38] consists of two main components: an encoder and a decoder, which jointly process the input sequence, based on the self-attention mechanism. Early works [26] adapted Transformers to the image domain. Even though this work demonstrated its ability only on very small images, it paved the way for broader works that addressed common challenges such as object detection [7] and classification [12]. Recently, several works [19,20] have been presented which show that Transformers can also be incorporated into the GAN architecture for image generation tasks. Unlike previous approaches, our method transfers motion between domains cyclically using unpaired data [48,3] and is based on attention in the temporal domain.

### 3 Method

CTrGAN differs in the following ways from CycleGAN and standard Transformer-based architecture. First, unlike CycleGAN, it cycles between domains by using a series of images rather than individual images. Second, unlike CycleGAN and Transformers, the attention is on the temporal domain between consecutive images and not between patches of the same image. This allows us to incorporate the target’s gait pattern into the source’s gait pattern transfer process. Third, we do not use positional encoding due to the approximate cyclic pattern of gait. Figure 2 depicts a schematic illustration of our Natural Gait Retargeting approach.

### 3.1 CTrGAN Architecture

The Cycle Transformer GAN (CTrGAN) consists of three main ingredients: features extractors, Transformers, and a cyclic process. We denote  $\mathcal{I} = \{\mathbf{I}_j\}_{j=1}^M$  as a collection of RGBA images and  $\mathcal{P} = \{\mathbf{P}_j\}_{j=1}^N$  as a collection of IUUV images [17].  $\mathbf{I}_j^{s_i}$ ,  $\mathbf{P}_j^{s_i}$  and  $\mathbf{I}_j^t$ ,  $\mathbf{P}_j^t$  denote the corresponding  $j^{th}$  image of the source and the target from the corresponding collection, respectively. In the following, we describe the details with respect to the target. Details regarding the source are derived in a similar manner. Below, the values in parenthesis represent those that we use in our implementation.

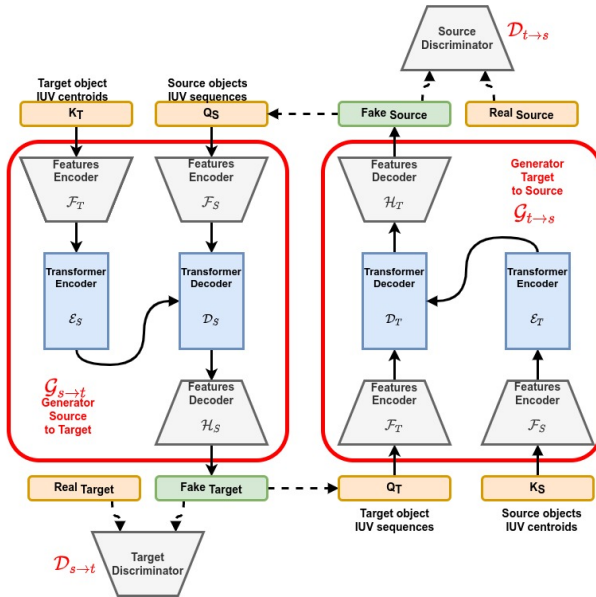


Fig. 3: Cycle Transformer GAN - CTrGAN

Fig. 4: CTrGAN consists of two branches that are connected cyclically, feature encoders and decoders and Transformers which perform self- and cross-attention between the features.

**Transformers.** The Transformers follow the same architecture as presented in [38]. Originally, Transformers were designed to handle sequences and consisted of two components, an encoder and a decoder. The encoder is designed to handle information that remains constant throughout the series, while the decoder is designed to handle the continuous flow of information. The encoder and decoder

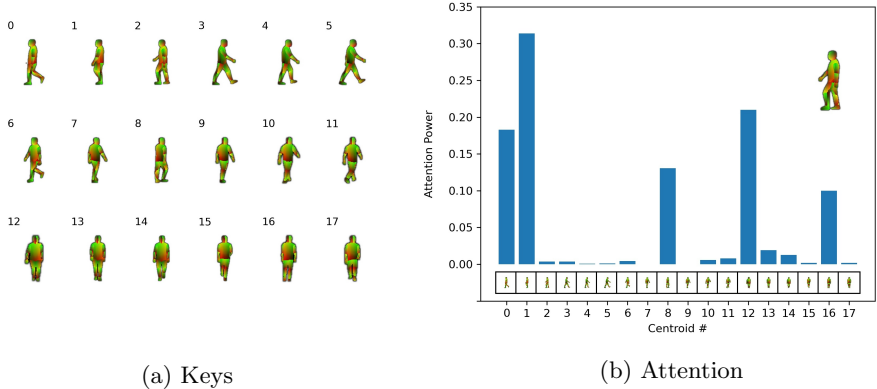


Fig. 5: (a) Samples of the Keys (centroids)  $\mathbf{K}_k^t$  that were used. (b) A visual demonstration of our attention mechanism.

consist of several chained attention blocks, and each receives three types of data as input: Keys, Values, and Queries (hereafter K, V and Q).

**Keys** The Keys of the target are selected from the images' collection whose feature vectors are the closest to the cluster centers. Let  $U_j$  denote the feature vector of image  $j$ :

$$\{\mathbf{U}_j\} = PCA(VGG_{16}(\{\mathbf{P}_j^t\}_{j=1..N}), d), \quad (1)$$

where  $VGG_{16}$  [33] are the features of the last layer (classifier) of the pre-trained VGG [27] and  $d$  is the PCA dimension ( $d = 100$ ).

$C_k$  denotes the center of the clusters as obtained by the K-means clustering:

$$\{\mathbf{C}_k\} = K_{means}(\{\mathbf{U}_j\}, m), \quad (2)$$

where  $m$  is the number of centroids ( $m = 18$ ). Finally, the Keys  $\{\mathbf{K}_k^t\}$  are defined as:

$$\mathbf{K}_k^t = \{\mathbf{P}_{p_k}^t\} \quad , \quad p_k = \{\operatorname{argmin}_j \|\mathbf{U}_j - \mathbf{C}_k\|_2\}. \quad (3)$$

Samples of the Keys that were used for one of the subjects can be seen in Figure 5a.

**Queries** Given an input sequence  $\mathbf{P}^t$ , the queries are a sliding window of  $l_w$  consecutive frames ( $l_w = 3$ ). We begin with a given frame and advance one sample at a time. During training, we choose a subsequence of length  $L$  at random and begin with its first frame. We process the entire series from beginning to end during inference.

**Features Encoders and Decoders** Given an IUVA image  $\mathbf{P}_j^t \in \mathbb{R}^{4 \times H \times W}$ , where IUVA is an IUV image with an additional alpha layer, we generate a feature tensor  $\mathbf{U}_j^t \in \mathbb{R}^{256 \times \frac{H}{64} \times \frac{W}{64}}$ . The feature encoder  $\mathcal{F}_T$  is a 5-layers CNN followed by 4 strides *max-pooling* (see Supplementary for more details).

The CTrGAN model includes two pairs of encoders ( $\mathcal{F}_T$  and  $\mathcal{F}_S$ ), where each of the pairs shares weights. All four feature encoders (shown in Figure 3) have the same structure. The  $\mathcal{H}_T$  and  $\mathcal{H}_S$  decoders are identical to the  $\mathcal{F}_T$  encoder, except that they operate in the other direction. The discriminators  $D_{t \rightarrow s}$  and  $D_{s \rightarrow t}$  (Figure 3) are 5-layers CNN (see Supplementary for more details).

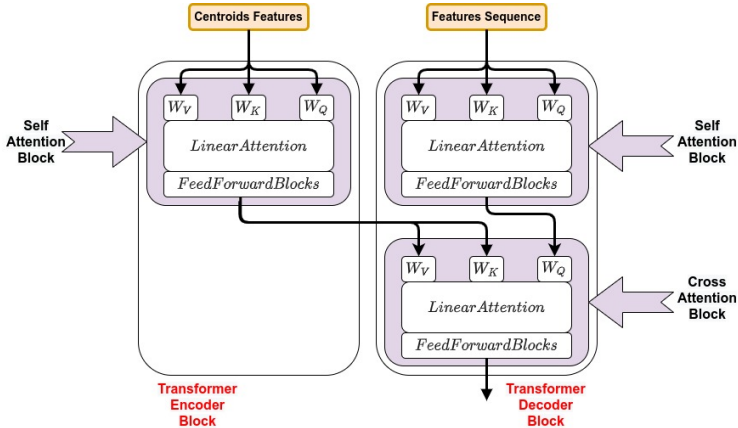


Fig. 6: Attention Layers. Left side - Transformer encoder. Right side - Transformer decoder. The encoder performs self-attention while the decoder performs self-attention followed by cross attention with the encoder’s outputs.

**Cycle Transformer GAN** Figure 3 shows the architecture of CTrGAN. We denote the source images collections as  $\Phi^{s_i} = \{\mathbf{I}^{s_i}, \mathbf{P}^{s_i}\}_{i=1..N}$  and the target image collection as  $\Psi^t = \{\mathbf{I}^t, \mathbf{P}^t\}$ . We define two networks  $\mathcal{G}_{s \rightarrow t}$  and  $\mathcal{G}_{t \rightarrow s}$ . The first network adapts pose images from a variety of sources to pose images of the target, while the second network does the opposite. We denote  $\tilde{\mathbf{P}}^t$  and  $\tilde{\mathbf{P}}^s$  as the outputs of the networks:

$$\{\tilde{\mathbf{P}}^t\} = \mathcal{G}_{s \rightarrow t} (\{\mathbf{K}^t\}, \{\mathbf{P}^{s_i}\}), \quad (4)$$

$$\{\tilde{\mathbf{P}}^{s_i}\} = \mathcal{G}_{t \rightarrow s} (\{\mathbf{K}^{s_i}\}, \{\mathbf{P}^t\}). \quad (5)$$

For brevity, images’ indices have been omitted. Using the pose images of the source’s gait pattern, our method attempts to generate pose images of the

target while preserving its gait pattern. This domain adaptation is accomplished by composing both  $\mathcal{G}_{s \rightarrow t}$  and  $\mathcal{G}_{t \rightarrow s}$  in a cyclic manner as shown in the following:

$$\tilde{\mathbf{P}}^{s_i} = \mathcal{G}_{t \rightarrow s}(\mathbf{K}^{s_i}, \mathcal{G}_{s \rightarrow t}(\mathbf{K}^t, \mathbf{P}^{s_i})), \quad (6)$$

$$\tilde{\mathbf{P}}^t = \mathcal{G}_{s \rightarrow t}(\mathbf{K}^t, \mathcal{G}_{t \rightarrow s}(\mathbf{K}^{s_i}, \mathbf{P}^t)). \quad (7)$$

The output pose image  $\tilde{\mathbf{P}}^t$  (i.e.  $\mathcal{G}_{s \rightarrow t}(\mathbf{K}^t, \mathbf{P}^{s_i})$ ) are used to generate the requested appearance by pose-to-appearance network  $\mathcal{G}_M$ :

$$\tilde{\mathbf{I}}_i^t = \mathcal{G}_M(\mathbf{P}_i^t). \quad (8)$$

**Self and Cross-Attention** The attention layer at the attention block is one of the core components of the Transformer. Its goal is to discover relationships between a given query  $Q$  (e.g. an image) and pre-exist key data  $K$  (e.g. a set of images) and to represent these relationships using  $V$ . It is stated as follows:

$$\text{Attention}(Q, K, V) = \text{Softmax}\left(\frac{Q, K^T}{\sqrt{d_k}}\right)V, \quad (9)$$

where  $d_k$  is a scaling factor [38].

Denote  $\mathcal{A}(Q, K, V)$  as the attention block (Eq. 9, see [38] for additional details) and denote  $\mathcal{F}_S$  and  $\mathcal{F}_T$  as the feature encoders of the source and target domains, respectively. The self attention of the Transformers encoders  $\mathcal{E}_S$  and  $\mathcal{E}_T$  and decoders  $\mathcal{D}_S$  and  $\mathcal{D}_T$  is:

$$\begin{aligned} \mathcal{E}_S(\mathbf{K}^t) &= \mathcal{A}(\mathcal{F}_T(\mathbf{K}^t), \mathcal{F}_T(\mathbf{K}^t), \mathcal{F}_T(\mathbf{K}^t)), \\ \mathcal{D}_S(\mathbf{P}^{s_i}) &= \mathcal{A}(\mathcal{F}_S(\mathbf{P}^{s_i}), \mathcal{F}_S(\mathbf{P}^{s_i}), \mathcal{F}_S(\mathbf{P}^{s_i})), \\ \mathcal{E}_T(\mathbf{K}^{s_i}) &= \mathcal{A}(\mathcal{F}_T(\mathbf{K}^{s_i}), \mathcal{F}_T(\mathbf{K}^{s_i}), \mathcal{F}_T(\mathbf{K}^{s_i})), \\ \mathcal{D}_T(\mathbf{P}^t) &= \mathcal{A}(\mathcal{F}_S(\mathbf{P}^t), \mathcal{F}_S(\mathbf{P}^t), \mathcal{F}_S(\mathbf{P}^t)). \end{aligned}$$

Note that the target's Keys  $\mathbf{K}^t$  Transformer encoders ( $\mathcal{E}_S$ ) remain unchanged throughout the training process whereas the source's keys  $\mathbf{K}^{s_i}$  (at  $\mathcal{E}_T$ ) are updated with accordance of the specific source that is currently being used for the cyclic training.

The generator of the source and target are cross attention operations:

$$\mathcal{G}_{s \rightarrow t}(\mathbf{K}^t, \mathbf{P}^{s_i}) = \mathcal{H}_S(\mathcal{A}(\mathcal{D}_S(\mathbf{P}^{s_i}), \mathcal{E}_S(\mathbf{K}^t), \mathcal{E}_S(\mathbf{K}^t))) \quad (10)$$

$$\mathcal{G}_{t \rightarrow s}(\mathbf{K}^{s_i}, \mathbf{P}^t) = \mathcal{H}_T(\mathcal{A}(\mathcal{D}_T(\mathbf{P}^t), \mathcal{E}_T(\mathbf{K}^{s_i}), \mathcal{E}_T(\mathbf{K}^{s_i}))), \quad (11)$$

where  $\mathcal{H}_S$  and  $\mathcal{H}_T$  are the features decoders of  $\mathcal{G}_{s \rightarrow t}$  and  $\mathcal{G}_{t \rightarrow s}$ , respectively.

Figure 6 illustrates the process of attention between the Transformer encoder and decoder. In order to reduce processing power, we use linear attention [21,35]

instead of Transformer’s original attention. Keys in the Transformer encoder undergo a process of attention among themselves and the output is served as the Keys and Values with the decoder’s queries. A self-attention process takes place between the decoder queries  $Q$  and themselves, which reveals temporal relationships between consecutive images. In our model, the Transformer decoder includes both self- and cross- attention blocks. We tested our model with and without using self-attention in the decoder and reported the results for both. Figure 5b visualizes the attention mechanism. More visualizations can be found in the Supplementary Materials.

### 3.2 Optimization and Loss Functions

We use the following loss functions in our training:

$$\ell_{cycle} = \lambda_{idt}\ell_{idt} + \lambda_{adv}\ell_{adv} + \lambda_{cyc}\ell_{cyc} + \lambda_{per}\ell_{per}, \quad (12)$$

where  $\lambda_{idt}$ ,  $\lambda_{adv}$ ,  $\lambda_{cyc}$  and  $\lambda_{per}$  are the weights of the losses. The identity loss function  $\ell_{idt}$  is used to ensure that the cyclic mapping preserves the mapping from a pose image to itself. We use  $\mathcal{L}_1$  loss function.

$$\ell_{idt} = \mathcal{L}_1(\mathcal{G}_{s \rightarrow t}(\mathbf{P}^t), \mathbf{P}^t) + \mathcal{L}_1(\mathcal{G}_{t \rightarrow s}(\mathbf{P}^s), \mathbf{P}^s). \quad (13)$$

Following CycleGAN [48] and ReCycleGAN [3] we use the same adversarial loss  $\ell_{adv}$ , in which two discriminator networks  $\mathcal{D}_{s \rightarrow t}$  and  $\mathcal{D}_{t \rightarrow s}$  are learned as a part of the training process.

In the same manner as GAN [16] architectures, we use the generator and discriminator  $\mathcal{G}_{s \rightarrow t}$ ,  $\mathcal{G}_{t \rightarrow s}$ ,  $\mathcal{D}_{s \rightarrow t}$  and  $\mathcal{D}_{t \rightarrow s}$ . In our training process, we use the  $\mathcal{L}_2$  as the objective loss function of the adversarial loss  $\ell_{adv}$ .

$$\begin{aligned} \ell_{adv} = & \mathcal{L}_2(\mathcal{D}_{s \rightarrow t}(\mathcal{G}_{s \rightarrow t}(\mathbf{P}^s)), \mathbf{0}) + \mathcal{L}_2(\mathcal{D}_{s \rightarrow t}(\mathbf{P}^t), \mathbf{1}) \\ & + \mathcal{L}_2(\mathcal{D}_{t \rightarrow s}(\mathcal{G}_{t \rightarrow s}(\mathbf{P}^t)), \mathbf{0}) + \mathcal{L}_2(\mathcal{D}_{t \rightarrow s}(\mathbf{P}^s), \mathbf{1}), \end{aligned} \quad (14)$$

where  $\mathbf{0}$  and  $\mathbf{1}$  are matrices of zeros and ones with the same dimensions as  $\mathcal{D}_{s \rightarrow t}(\mathcal{G}_{s \rightarrow t}(\mathbf{P}^s))$  and  $\mathcal{D}_{t \rightarrow s}(\mathcal{G}_{t \rightarrow s}(\mathbf{P}^t))$ .

The cycle loss function  $\ell_{cyc}$  which is the main core of the cycle GAN process is defined as:

$$\ell_{cyc} = \mathcal{L}_2(\mathcal{G}_{t \rightarrow s}(\mathcal{G}_{s \rightarrow t}(\mathbf{P}^s)), \mathbf{P}^s) + \mathcal{L}_2(\mathcal{G}_{s \rightarrow t}(\mathcal{G}_{t \rightarrow s}(\mathbf{P}^t)), \mathbf{P}^t). \quad (15)$$

The perceptual loss  $\ell_{per}$  measures the difference between feature vectors of a real image and a generated one:

$$\begin{aligned} \ell_{per} = & \mathcal{L}_1(VGG_{16}(\mathcal{G}_{t \rightarrow s}(\mathcal{G}_{s \rightarrow t}(\mathbf{P}^s))), VGG_{16}(\mathbf{P}^s)) \\ & + \mathcal{L}_1(VGG_{16}(\mathcal{G}_{s \rightarrow t}(\mathcal{G}_{t \rightarrow s}(\mathbf{P}^t))), VGG_{16}(\mathbf{P}^t)). \end{aligned} \quad (16)$$

We use a pre-trained VGG model [33,27] to extract the feature vectors. VGG model is pre-trained on three layers of RGB, whereas we use four layers (IUVA), we therefore measured the perceptual loss of the IUVA and the alpha channels separately.

## 4 Experiments

### 4.1 Dataset

We use CASIA-A [39], which is a widely-used gait recognition dataset [22,13,1,31]. It includes twenty subjects. Each subject has twelve image sequences that were captured from three different viewpoints, resulting in four instances for each of the viewpoints (denoted by 001, 002, 003 and 004). Overall, there are a total of 240 video sequences with a resolution of 352x240 and 19,139 images.



Fig. 7: Pre-processing procedure - From left to right: 1. Original image. 2. Cropped and centered image. 3. Pose image (IUV - DensePose format). 4. Masked image, created from the I part of the IUV image

We removed the background from the original CASIA-A images by using DensePose [17]. The input to our model is four-channel images (RGBA). In each frame, we extracted the binary mask for the subject and attached it to the RGB image as an alpha channel. The images were cropped and centered around the object to create 256x256 canvases. See Figure 7 for examples.

### 4.2 Implementation Details

The networks were implemented using Pytorch [27] and trained on a single NVidia 2080Ti GPU. We trained the model with Adam optimizer with  $\beta_1 = 0.5$   $\beta_2 = 0.999$  over 20 epochs. The initial learning rate was set to  $2e - 4$ , for 5 epochs followed by a linear decay to zero over 15 more epochs. The same configurations and parameters were used for all models ( $\mathcal{F}_T, \mathcal{F}_S, \mathcal{H}_T, \mathcal{H}_S, \mathcal{E}_S, \mathcal{D}_S, \mathcal{E}_T, \mathcal{D}_T$  and  $\mathcal{D}_{s \rightarrow t}, \mathcal{D}_{t \rightarrow s}$ ). In order to represent temporal relations more effectively, we used three consecutive frames as a mini-batch. Our augmentations included a small magnification (from 256 to 272) and random cropping.

A detailed description of our architecture can be found in the Supplementary Materials.

### 4.3 Baselines

The baselines are state-of-the-art methods for motion retargeting, V2V [41] and EDN [8]. The models have been adapted to include an alpha channel as well.

EDN has been adjusted to work with IUVA (IUV + alpha channel), whereas the V2V model is already optimized for DensePose images, so only one more channel is needed. V2V and EDN were trained according to their protocol with the default parameters.

We evaluate the following approaches to assess CTrGAN’s contribution: (a) direct - using trained baselines to map directly from pose to appearance. (b) ours - we use CTrGAN to generate the pose images, then use the baselines to render the appearance.

#### 4.4 Metrics

**Gait quality.** We evaluate our results by gait recognition models GaitSet [9], GaitGL [25] and GaitPart [14], implemented by the OpenGait [15] package.

Given a set of reference videos  $\{\mathbf{I}^{s_i}\}$  and a generated video  $\mathbf{I}^g$ , the goal is to find the reference video in which the gait pattern is the most similar. For that, references videos are ranked according to their distance from  $\mathbf{I}^g$ :

$$D_{s_i,g} = \|\mathcal{M}(\mathbf{I}^{s_i}) - \mathcal{M}(\mathbf{I}^g)\|_2, \quad (17)$$

where  $\mathcal{M}$  is the specific model. The most similar reference video is considered as the one with the highest top-3 (minimum distance) frequency  $\mathbf{I}^{s_i^*}$ . The identified gait is of the subject in  $\mathbf{I}^{s_i^*}$  and the recovered distance is  $D_{s_i^*,g}$ . In our case the generated video  $\mathbf{I}^g$  is  $\mathcal{G}_M(\mathcal{G}_{s \rightarrow t}(\mathbf{P}^g))$ , where  $\mathcal{G}_M$  is the pose to appearance model that is in use (*e.g.* V2V).

We report **target-accuracy** - the percentages of times the gait recognition model has identified the generated gait as the target’s gait.

The models were trained on all the subjects and half of the CASIA-A videos.

**Appearance quality.** We used the following metrics to evaluate our appearance quality: Inception Score (IS)[30], Structural Similarity (SSIM) [43], Perceptual Image Patch Similarity (LPIPS), [47] and Frechet Inception Distance (FID) [18].

FID and IS metrics measure statistical differences between sets of images and not directly between individual images. However, SSIM and LPIPS evaluate the generated image based on a single, ground truth image. Due to the fact that the generated synthetic image  $\tilde{\mathbf{I}}_i^t$  in our test set can be derived from an unseen source’s pose, a ground-truth image  $\mathbf{I}_i^t$  is not always available. We therefore use the Chamfer Distance [4] to recover the nearest ground truth image from the reference video sequence  $\{\mathbf{I}_k^r\}$ :

$$E_{CD} = \frac{1}{N} \sum_{i=1}^N \min_k Q(\tilde{\mathbf{I}}_i^t, \mathbf{I}_k^r), \quad (18)$$

where  $Q$  represents our quality metrics, SSIM or LPIPS. All methods were compared using  $E_{CD}$ , both ours and others.

Table 1: The target-accuracy  $\uparrow$ . Each number is the percentage of times the gait recondition model has identified the generated gait as the target’s gait. The top row is before and the bottom row is after applying CTrGAN to generate the poses. Our approach significantly improves the ability to generate the target’s gait, up to approximately  $\times 21$  than existing methods (GaitPart+V2V).

Method	Model	GaitPart	GaitSet	GaitGL
-	EDN	16.94	29.44	16.67
	V2V	3.89	3.61	4.17
ours	EDN	18.89	<b>62.78</b>	36.39
	V2V	<b>84.72</b>	56.67	<b>68.06</b>

## 4.5 Results

**CTrGAN successfully generates the gait of the target.** We trained our model on thirteen subjects and use the remaining seven for testing. We left out of the training set two video sequences (out of four) for each subject and include them in the test set. In this way, we have been able to include cases in which sources were available or unavailable during training in our evaluation.

For the test set, we generated video sequences for the trained subjects. We deployed all subjects in the dataset as sources, including those not included in the training set. We tested the ability to identify the generated gait as the target’s gait by the gait recognition models, before and after applying our approach. Our results demonstrate that our approach can generate a more realistic gait for the target by an order of magnitude than previous methods.

Table 1 presents the target-accuracy obtained by the gait recognition models. In all the tables, bold represents the best result. The top of the table shows the baselines applied directly to the pose of the source. At the bottom of the table, CTrGAN generates the poses of the target before applying the baseline methods. It can be seen that for all the methods, CTrGAN significantly improves the ability to generate the natural gait of the target. All models have failed to recognize the gait of the target in the case of V2V without CTrGAN. This implies that indeed, V2V can accurately mimic the movements of the source by the target, in accordance with its original goal. On average, the generated gait rendered by V2V is approximately 17 times more likely to match the target’s gait when using our method.

Figure 8 shows the distances obtained by GaitSet for subject number three (the target) with respect to all the twenty subjects in the test set (the sources). Dark colors represent low values, whereas light colors represent high values. The lower the distance, the more similar the gait in the reference sequence is to that in the generated sequence. Figure 8a presents the distance matrix for the V2V method in the direct approach. It can be seen that GaitSet has been able to accurately recognize the sources for all the generated sequences. Figure 8b presents the results for V2V after applying our CTrGAN to generate the poses.



Fig. 8: GaitSet’s distance matrix for subject three (the target) in the training set before and after applying our method. The darker the color the lower the value. It can be seen that before deploying our model, GaitSet easily distinguishes between the generated and real gait and can identify the true sources. After applying our approach, GaitSet identifies for most of the cases the generated gait as the real gait of subject three.

Table 2: Appearance quality.

Method	Model	SSIM [CD] $\uparrow$	LPIPS [CD] $\downarrow$	FID $\downarrow$	IS $\downarrow$
-	EDN	0.890	0.072	55.79	0.0025
	V2V	0.901	0.063	53.131	0.0010
ours	EDN	0.870	0.101	83.67	0.0030
	V2V	<b>0.909</b>	<b>0.055</b>	<b>52.89</b>	<b>0.0009</b>

For the vast majority of the sequences, GaitSet has recognized the generated gait of the target (subject three) as the real gait.

Table 2 shows the appearance quality of the different approaches, with and without CTrGAN. Deploying pose to appearance networks directly without CTrGAN, the obtained appearance metrics are similar across the different methods. Using CTrGAN slightly increases the appearance quality for V2V. It is expected as the key contribution of CTrGAN is the generation of poses that can naturally be attributed to the target rather than improving the rendering mechanism of an existing pose. A possible explanation for the slight improvement could be that the generated poses by CTrGAN match more naturally the target’s appearances that need to be rendered.

**Motion transfer mimics the gait of the source.** Here, we examine the extent to which existing methods retain the gait pattern of the source after applying the gait transfer.

Table 3 presents the source-accuracy. It is defined as the percentage of times the gait recognition model has identified the generated gait as the source’s gait. The top of the table shows that the models correctly identified the sources after

Table 3: The source-accuracy ↓.

Method	Model	GaitPart	GaitSet	GaitGL
-	EDN	17.22	20.28	47.78
	V2V	93.06	76.94	93.33
ours	EDN	<b>7.78</b>	<b>7.22</b>	<b>12.78</b>
	V2V	9.44	15.00	20.56

generating the target’s appearance in about 87 percent of the test cases, illustrating the challenge of present motion transfer methods to generate gait distinguishable from the source. The bottom of the table shows that, with CTrGAN, the gait recognition models’ success rate drops significantly to approximately 15 percent of cases.

**The contribution of temporal attention.** Table 4 shows the effect of the different components of CTrGAN on the final results, tested on V2V as our pose to appearance network. It can be seen that CycleGAN architecture on its own is not sufficient in order to generate natural poses of the target. Adding encoder self-attention and cross-attention between the image sequence and the keys using the decoder produces significantly more natural poses, with respect to all gait recognition models. A further improvement is obtained when the decoder self-attention is added, which takes advantage of the temporal relations within the sequence. Additional detailed comparisons can be found in the Supplementary Materials.

Table 4: The target recognition accuracy of several CTrGAN configurations. V2V was used as the pose to appearance model.

Model	Features			Gait scores		
	Attention mechanism	Encoder self-attention	Decoder self-attention	GaitSet	GaitGL	GaitPart
Cycle Only	✗	✗	✗	5.00	5.28	5.56
+ Attention	✓	✓	✗	51.39	69.17	78.06
+ Time-Attention	✓	✓	✓	56.67	68.06	84.72

## 5 Conclusion

We investigate the gait retargeting problem. We have shown that current state-of-the-art approaches are unable to produce natural gaits for the targets. Our approach to this problem is to introduce CTrGAN, a transformer-based architecture that can be used to perform synthesis tasks involving unpaired data

and temporal relationships. Our study demonstrated that CTrGAN can produce poses of the target based on sources other than those in the training set such that state-of-the-art gait recognition models consider the poses to be the natural gait of the target.

## References

1. Arantes, M., Gonzaga, A.: Human gait recognition using extraction and fusion of global motion features. *Multimedia Tools and Applications* **55**, 655–675 (2010)
2. Averbuch-Elor, H., Cohen-Or, D., Kopf, J., Cohen, M.F.: Bringing portraits to life. *ACM Transactions on Graphics (TOG)* **36**(6), 1–13 (2017)
3. Bansal, A., Ma, S., Ramanan, D., Sheikh, Y.: Recycle-gan: Unsupervised video re-targeting. In: Ferrari, V., Hebert, M., Sminchisescu, C., Weiss, Y. (eds.) *Computer Vision - ECCV 2018 - 15th European Conference, Munich, Germany, September 8-14, 2018, Proceedings, Part V. Lecture Notes in Computer Science*, vol. 11209, pp. 122–138. Springer (2018). [https://doi.org/10.1007/978-3-030-01228-1\\_8](https://doi.org/10.1007/978-3-030-01228-1_8), [https://doi.org/10.1007/978-3-030-01228-1\\_8](https://doi.org/10.1007/978-3-030-01228-1_8)
4. Barrow, H.G., Tenenbaum, J.M., Bolles, R.C., Wolf, H.C.: Parametric correspondence and chamfer matching: Two new techniques for image matching. In: *IJCAI*. pp. 659–663 (1977), <http://ijcai.org/Proceedings/77-2/Papers/024.pdf>
5. Brown, T., Mann, B., Ryder, N., Subbiah, M., Kaplan, J.D., Dhariwal, P., Neelakantan, A., Shyam, P., Sastry, G., Askell, A., Agarwal, S., Herbert-Voss, A., Krueger, G., Henighan, T., Child, R., Ramesh, A., Ziegler, D., Wu, J., Winter, C., Hesse, C., Chen, M., Sigler, E., Litwin, M., Gray, S., Chess, B., Clark, J., Berner, C., McCandlish, S., Radford, A., Sutskever, I., Amodei, D.: Language models are few-shot learners. In: Larochelle, H., Ranzato, M., Hadsell, R., Balcan, M.F., Lin, H. (eds.) *Advances in Neural Information Processing Systems*. vol. 33, pp. 1877–1901. Curran Associates, Inc. (2020)
6. Cao, Z., Simon, T., Wei, S.E., Sheikh, Y.: Realtime multi-person 2d pose estimation using part affinity fields. In: *Proceedings of the IEEE conference on computer vision and pattern recognition*. pp. 7291–7299 (2017)
7. Carion, N., Massa, F., Synnaeve, G., Usunier, N., Kirillov, A., Zagoruyko, S.: End-to-end object detection with transformers. In: Vedaldi, A., Bischof, H., Brox, T., Frahm, J. (eds.) *Computer Vision - ECCV 2020 - 16th European Conference, Glasgow, UK, August 23-28, 2020, Proceedings, Part I. Lecture Notes in Computer Science*, vol. 12346, pp. 213–229. Springer (2020). [https://doi.org/10.1007/978-3-030-58452-8\\_13](https://doi.org/10.1007/978-3-030-58452-8_13), [https://doi.org/10.1007/978-3-030-58452-8\\_13](https://doi.org/10.1007/978-3-030-58452-8_13)
8. Chan, C., Ginosar, S., Zhou, T., Efros, A.A.: Everybody dance now. In: *IEEE International Conference on Computer Vision (ICCV)* (2019)
9. Chao, H., He, Y., Zhang, J., Feng, J.: Gaitset: Regarding gait as a set for cross-view gait recognition. In: *The Thirty-Third AAAI Conference on Artificial Intelligence, AAAI 2019, The Thirty-First Innovative Applications of Artificial Intelligence Conference, IAAI 2019, The Ninth AAAI Symposium on Educational Advances in Artificial Intelligence, EAAI 2019, Honolulu, Hawaii, USA, January 27 - February 1, 2019*. pp. 8126–8133. AAAI Press (2019). <https://doi.org/10.1609/aaai.v33i01.33018126>, <https://doi.org/10.1609/aaai.v33i01.33018126>
10. Cormier, M., Moshkenan, H.M., Lörch, F., Metzler, J., Beyerer, J.: Do as we do: Multiple person video-to-video transfer. In: *4th IEEE International Conference on Multimedia Information Processing and Retrieval*,

- MIPR 2021, Tokyo, Japan, September 8-10, 2021. pp. 84–90. IEEE (2021). <https://doi.org/10.1109/MIPR51284.2021.00020>, <https://doi.org/10.1109/MIPR51284.2021.00020>
11. Cosma, A., Radoi, I.E.: Wildgait: Learning gait representations from raw surveillance streams. *Sensors* **21**(24), 8387 (2021). <https://doi.org/10.3390/s21248387>, <https://doi.org/10.3390/s21248387>
  12. Dosovitskiy, A., Beyer, L., Kolesnikov, A., Weissenborn, D., Zhai, X., Unterthiner, T., Dehghani, M., Minderer, M., Heigold, G., Gelly, S., Uszkoreit, J., Houlsby, N.: An image is worth 16x16 words: Transformers for image recognition at scale. In: 9th International Conference on Learning Representations, ICLR 2021, Virtual Event, Austria, May 3-7, 2021. OpenReview.net (2021), <https://openreview.net/forum?id=YicbFdNTTY>
  13. Ekinci, M., Aykut, M.: Human identification using gait. 2006 IEEE 14th Signal Processing and Communications Applications pp. 1–4 (2006)
  14. Fan, C., Peng, Y., Cao, C., Liu, X., Hou, S., Chi, J., Huang, Y., Li, Q., He, Z.: Gaitpart: Temporal part-based model for gait recognition. In: 2020 IEEE/CVF Conference on Computer Vision and Pattern Recognition, CVPR 2020, Seattle, WA, USA, June 13-19, 2020. pp. 14213–14221. Computer Vision Foundation / IEEE (2020). <https://doi.org/10.1109/CVPR42600.2020.01423>
  15. Fan, C., Shen, C., Liang, J.: Opengait. <https://github.com/ShiqiYu/OpenGait> (2022)
  16. Goodfellow, I., Pouget-Abadie, J., Mirza, M., Xu, B., Warde-Farley, D., Ozair, S., Courville, A., Bengio, Y.: Generative adversarial nets. In: Ghahramani, Z., Welling, M., Cortes, C., Lawrence, N., Weinberger, K.Q. (eds.) *Advances in Neural Information Processing Systems*. vol. 27. Curran Associates, Inc. (2014), <https://proceedings.neurips.cc/paper/2014/file/5ca3e9b122f61f8f06494c97b1afccf3-Paper.pdf>
  17. Güler, R.A., Neverova, N., Kokkinos, I.: Densepose: Dense human pose estimation in the wild. In: 2018 IEEE Conference on Computer Vision and Pattern Recognition, CVPR 2018, Salt Lake City, UT, USA, June 18-22, 2018. pp. 7297–7306. Computer Vision Foundation / IEEE Computer Society (2018). <https://doi.org/10.1109/CVPR.2018.00762>
  18. Heusel, M., Ramsauer, H., Unterthiner, T., Nessler, B., Hochreiter, S.: Gans trained by a two time-scale update rule converge to a local nash equilibrium. In: Guyon, I., von Luxburg, U., Bengio, S., Wallach, H.M., Fergus, R., Vishwanathan, S.V.N., Garnett, R. (eds.) *Advances in Neural Information Processing Systems 30: Annual Conference on Neural Information Processing Systems 2017*, December 4-9, 2017, Long Beach, CA, USA. pp. 6626–6637 (2017)
  19. Hudson, D.A., Zitnick, L.: Generative adversarial transformers. In: Meila, M., Zhang, T. (eds.) *Proceedings of the 38th International Conference on Machine Learning, ICML 2021*, 18-24 July 2021, Virtual Event. *Proceedings of Machine Learning Research*, vol. 139, pp. 4487–4499. PMLR (2021), <http://proceedings.mlr.press/v139/hudson21a.html>
  20. Jiang, Y., Chang, S., Wang, Z.: Transgan: Two pure transformers can make one strong gan, and that can scale up. *Advances in Neural Information Processing Systems* **34** (2021)
  21. Katharopoulos, A., Vyas, A., Pappas, N., Fleuret, F.: Transformers are rnns: Fast autoregressive transformers with linear attention. In: *Proceedings of the 37th International Conference on Machine Learning, ICML 2020*, 13-18 July 2020, Virtual Event. *Proceedings of Machine Learning Research*, vol. 119, pp. 5156–5165. PMLR (2020), <http://proceedings.mlr.press/v119/katharopoulos20a.html>

22. Khan, M.H., Li, F., Farid, M.S., Grzegorzec, M.: Gait recognition using motion trajectory analysis. In: Kurzynski, M., Wozniak, M., Burduk, R. (eds.) Proceedings of the 10th International Conference on Computer Recognition Systems CORES 2017, Polanica Zdroj, Poland, 22-24 May 2017. Advances in Intelligent Systems and Computing, vol. 578, pp. 73–82 (2017). [https://doi.org/10.1007/978-3-319-59162-9\\_8](https://doi.org/10.1007/978-3-319-59162-9_8), [https://doi.org/10.1007/978-3-319-59162-9\\_8](https://doi.org/10.1007/978-3-319-59162-9_8)
23. Kim, H., Garrido, P., Tewari, A., Xu, W., Thies, J., Niessner, M., Pérez, P., Richardt, C., Zollhöfer, M., Theobalt, C.: Deep video portraits. *ACM Transactions on Graphics (TOG)* **37**(4), 1–14 (2018)
24. Li, Y., Chang, M.C., Lyu, S.: In ictu oculi: Exposing ai generated fake face videos by detecting eye blinking (2018)
25. Lin, B., Zhang, S., Yu, X.: Gait recognition via effective global-local feature representation and local temporal aggregation. In: Proceedings of the IEEE/CVF International Conference on Computer Vision (ICCV). pp. 14648–14656 (October 2021)
26. Parmar, N.J., Vaswani, A., Uszkoreit, J., Kaiser, L., Shazeer, N., Ku, A., Tran, D.: Image transformer. In: International Conference on Machine Learning (ICML) (2018), <http://proceedings.mlr.press/v80/parmar18a.html>
27. Paszke, A., Gross, S., Massa, F., Lerer, A., Bradbury, J., Chanan, G., Killeen, T., Lin, Z., Gimelshein, N., Antiga, L., Desmaison, A., Kopf, A., Yang, E., DeVito, Z., Raison, M., Tejani, A., Chilamkurthy, S., Steiner, B., Fang, L., Bai, J., Chintala, S.: Pytorch: An imperative style, high-performance deep learning library. In: Wallach, H., Larochelle, H., Beygelzimer, A., d'Alché-Buc, F., Fox, E., Garnett, R. (eds.) Advances in Neural Information Processing Systems 32, pp. 8024–8035. Curran Associates, Inc. (2019), <http://papers.neurips.cc/paper/9015-pytorch-an-imperative-style-high-performance-deep-learning-library.pdf>
28. Ren, J., Chai, M., Tulyakov, S., Fang, C., Shen, X., Yang, J.: Human motion transfer from poses in the wild. In: European Conference on Computer Vision. pp. 262–279. Springer (2020)
29. Sabir, E., Cheng, J., Jaiswal, A., AbdAlmageed, W., Masi, I., Natarajan, P.: Recurrent convolutional strategies for face manipulation detection in videos (2019)
30. Salimans, T., Goodfellow, I., Zaremba, W., Cheung, V., Radford, A., Chen, X., Chen, X.: Improved techniques for training gans. In: Lee, D., Sugiyama, M., Luxburg, U., Guyon, I., Garnett, R. (eds.) Advances in Neural Information Processing Systems. vol. 29. Curran Associates, Inc. (2016)
31. Filipi Gonçalves dos Santos, C., Oliveira, D.d.S., A. Passos, L., Gonçalves Pires, R., Felipe Silva Santos, D., Pascotti Valem, L., P. Moreira, T., Cleison S. Santana, M., Roder, M., Paulo Papa, J., Colombo, D.: Gait recognition based on deep learning: A survey. *ACM Comput. Surv.* **55**(2) (jan 2022). <https://doi.org/10.1145/3490235>, <https://doi.org/10.1145/3490235>
32. Siarohin, A., Lathuilière, S., Tulyakov, S., Ricci, E., Sebe, N.: Animating arbitrary objects via deep motion transfer. In: IEEE Conference on Computer Vision and Pattern Recognition, CVPR 2019, Long Beach, CA, USA, June 16-20, 2019. pp. 2377–2386. Computer Vision Foundation / IEEE (2019). <https://doi.org/10.1109/CVPR.2019.00248>
33. Simonyan, K., Zisserman, A.: Very deep convolutional networks for large-scale image recognition. In: International Conference on Learning Representations (2015)
34. Singh, J.P., Jain, S., Arora, S., Singh, U.P.: Vision-based gait recognition: A survey. *IEEE Access* **6**, 70497–70527 (2018)

35. Sun, J., Shen, Z., Wang, Y., Bao, H., Zhou, X.: Loftr: Detector-free local feature matching with transformers. In: IEEE Conference on Computer Vision and Pattern Recognition, CVPR 2021, virtual, June 19-25, 2021. pp. 8922–8931. Computer Vision Foundation / IEEE (2021), [https://openaccess.thecvf.com/content/CVPR2021/html/Sun\\_LoFTR\\_Detector-Free\\_Local\\_Feature\\_Matching\\_With\\_Transformers\\_CVPR\\_2021\\_paper.html](https://openaccess.thecvf.com/content/CVPR2021/html/Sun_LoFTR_Detector-Free_Local_Feature_Matching_With_Transformers_CVPR_2021_paper.html)
36. Teepe, T., Khan, A., Gilg, J., Herzog, F., Hörmann, S., Rigoll, G.: Gaitgraph: Graph convolutional network for skeleton-based gait recognition. In: 2021 IEEE International Conference on Image Processing, ICIP 2021, Anchorage, AK, USA, September 19-22, 2021. pp. 2314–2318. IEEE (2021). <https://doi.org/10.1109/ICIP42928.2021.9506717>, <https://doi.org/10.1109/ICIP42928.2021.9506717>
37. Thies, J., Zollhofer, M., Stamminger, M., Theobalt, C., Nießner, M.: Face2face: Real-time face capture and reenactment of rgb videos. In: Proceedings of the IEEE conference on computer vision and pattern recognition. pp. 2387–2395 (2016)
38. Vaswani, A., Shazeer, N., Parmar, N., Uszkoreit, J., Jones, L., Gomez, A.N., Kaiser, L.u., Polosukhin, I.: Attention is all you need. In: Guyon, I., Luxburg, U.V., Bengio, S., Wallach, H., Fergus, R., Vishwanathan, S., Garnett, R. (eds.) Advances in Neural Information Processing Systems. vol. 30. Curran Associates, Inc. (2017)
39. Wang, L., Tan, T., Ning, H., Hu, W.: Silhouette analysis-based gait recognition for human identification. IEEE Trans. Pattern Anal. Mach. Intell. **25**(12), 1505–1518 (2003). <https://doi.org/10.1109/TPAMI.2003.1251144>, <https://doi.org/10.1109/TPAMI.2003.1251144>
40. Wang, T.C., Liu, M.Y., Tao, A., Liu, G., Kautz, J., Catanzaro, B.: Few-shot video-to-video synthesis. In: Advances in Neural Information Processing Systems (NeurIPS) (2019)
41. Wang, T.C., Liu, M.Y., Zhu, J.Y., Liu, G., Tao, A., Kautz, J., Catanzaro, B.: Video-to-video synthesis. In: Conference on Neural Information Processing Systems (NeurIPS) (2018)
42. Wang, T.C., Liu, M.Y., Zhu, J.Y., Tao, A., Kautz, J., Catanzaro, B.: High-resolution image synthesis and semantic manipulation with conditional gans. In: Proceedings of the IEEE conference on computer vision and pattern recognition. pp. 8798–8807 (2018)
43. Wang, Z., Bovik, A.C., Sheikh, H.R., Simoncelli, E.P.: Image quality assessment: from error visibility to structural similarity. IEEE Trans. Image Process. **13**(4), 600–612 (2004). <https://doi.org/10.1109/TIP.2003.819861>, <https://doi.org/10.1109/TIP.2003.819861>
44. Wolf, T., Debut, L., Sanh, V., Chaumond, J., Delangue, C., Moi, A., Cistac, P., Rault, T., Louf, R., Funtowicz, M., Davison, J., Shleifer, S., von Platen, P., Ma, C., Jernite, Y., Plu, J., Xu, C., Le Scao, T., Gugger, S., Drame, M., Lhoest, Q., Rush, A.: Transformers: State-of-the-art natural language processing. In: Proceedings of the 2020 Conference on Empirical Methods in Natural Language Processing: System Demonstrations. pp. 38–45. Association for Computational Linguistics, Online (Oct 2020). <https://doi.org/10.18653/v1/2020.emnlp-demos.6>, <https://aclanthology.org/2020.emnlp-demos.6>
45. Wu, K., Yin, C., Che, Z., Jiang, B., Tang, J., Guan, Z., Ding, G.: Human pose transfer with disentangled feature consistency. arXiv preprint arXiv:2107.10984 (2021)
46. Zhang, B., Gu, S., Zhang, B., Bao, J., Chen, D., Wen, F., Wang, Y., Guo, B.: Styleswin: Transformer-based GAN for high-resolution image generation. CoRR **abs/2112.10762** (2021), <https://arxiv.org/abs/2112.10762>

47. Zhang, R., Isola, P., Efros, A.A., Shechtman, E., Wang, O.: The unreasonable effectiveness of deep features as a perceptual metric. In: 2018 IEEE Conference on Computer Vision and Pattern Recognition, CVPR 2018, Salt Lake City, UT, USA, June 18-22, 2018. pp. 586–595. Computer Vision Foundation / IEEE Computer Society (2018). <https://doi.org/10.1109/CVPR.2018.00068>
48. Zhu, J.Y., Park, T., Isola, P., Efros, A.A.: Unpaired image-to-image translation using cycle-consistent adversarial networks. In: Computer Vision (ICCV), 2017 IEEE International Conference on (2017)